

Study of kinetics of magnetic permeability aftereffect in amorphous $\text{Co}_{70.4}\text{Fe}_{4.6}\text{Si}_{15}\text{B}_{10}$

S. P. Cruz f. *, M. Knobel, J. P. Sinnecker and R. Sato Turtelli
Instituto de Física, UNICAMP, LMBT, Caixa Postal 6165, Campinas, 13081, SP, Brasil

Received August 30, 1990

Abstract Initial permeability aftereffect measurements have been performed on three sets of amorphous $\text{Co}_{70.4}\text{Fe}_{4.6}\text{Si}_{15}\text{B}_{10}$ alloys produced with different quenching rates. We have carried out isothermal annealings of **as-cast** samples with and without longitudinal magnetic field applied ($H=180$ G) for temperatures 473K and **573K**. The annealing kinetics of the aftereffect can be understood in **terms** of a competition between two different relaxation processes, the compositional and the topological short range ordering. Both these processes are influenced by the quenching rate.

1. Introduction

The magnetic relaxation and the structural instability of amorphous metal-metalloid alloys are the main obstacles for a wider exploitation of their excellent magnetic characteristics. The study of the magnetic relaxation and its stability is important not only for technological applications, but also in order to understand the behavior of atomic rearrangement during structural relaxation.

One of the most adequate techniques to perform this study is the so called initial magnetic permeability aftereffect, due to its great sensitivity to structural changes. The aftereffect of the magnetic permeability originates from a **progressive** damping of domain-wall motion after any domain-wall rearrangement. This damping comes from the reorientation of mobile atom pairs or, more generally, from **small** atomic clusters, usually pictured as magnetic defects randomly distributed within the material and interacting with the local magnetization direction within each **domain-wall**^{1,2}. Although the nature of this interaction is **still**

* On leave from Pontifícia Universidade Católica, Porto Alegre

Study of kinetics of magnetic permeability...

rather controversial^{2,3}, the directional ordering is generally assumed to be characterized by an extended range of activation energies, with relaxation times obeying Arrhenius law.

It has been observed that the as-cast atomic disorder degree frozen into the material depends on the quenching rate (QR) at which the material is produced^{4,5}. Higher QR always corresponds to more disordered amorphous structures⁶. A good correlation indeed exists among the QR, the initial permeability aftereffect¹⁻⁴ and the electrical resistivity (ρ)⁵. Values of such quantities at room temperature and their changes with annealing, attributed to structural relaxation, are dependent on the disorder degree of the alloys. The relaxation of these properties occurs with lower activation energies in fast-quenched alloys⁷.

There are indications that different types of short-range ordering processes are simultaneously present in as-cast amorphous alloys submitted to annealing. These are the topological short-range ordering (TSRO)⁸ and chemical short-range ordering (CSRO)⁹. The TSRO is responsible for the structural relaxation and involves irreversible annihilation of free volume¹⁰. The CSRO is related to directional order for pairs of magnetic atoms, which can be almost completely reversible⁸.

The present work reports the influence of isothermal annealing treatments on the initial magnetic permeability aftereffect and on the permeability itself. Three sets of amorphous samples, of the same composition and produced with different QR, are analyzed. The behavior of the measured aftereffect as a function of annealing time can be understood in terms of a competition between the different relaxation processes that take place in the amorphous bulk during the thermal treatment. The kinetics of the relaxation phenomena in amorphous alloys depends upon annealing conditions and allows us to obtain information about the effect of different free volume content on the TSRO and CSRO processes.

2. Experimental

Magnetic permeability aftereffect and permeability were measured at room temperature as a function of annealing time in three sets (A,B and C) of nearly zero

S. P. Cruz f., M. Knobel, J. P. Sinnecker and R. Sato Turtelli

magnetostrictive amorphous $\text{Co}_{70.4}\text{Fe}_{4.6}\text{Si}_{15}\text{B}_{10}$ samples prepared with different QR by single-roller melt spinning in air.

The magnetic permeability aftereffect $((\Delta\mu/\mu).He)$ was measured by means of the standard impulsive technique¹¹ between the fixed times $t_1 = 1s$ and $t_2 = 11s$. After a rapid magnetic pulse ($\cong 10^{-5}$ s, 2 G) the subsequent permeability decay was measured by a lock-in amplifier. The amplitude of the 90 KHz drive field (He) was chosen in order to give a maximum in the μ vs. $\Delta\mu$ curve². Owing to the displacements of the position of this maximum with aging time t, the amplitude of He has varied between 1.0 and 2.0 A/m.

The permeability (μ) was obtained from the magnetic induction (B) measurements in the linear region of the B vs. H curve.

The samples were submitted to annealing in Ar atmosphere at $T_a = 473K$ with and without an applied longitudinal D.C. magnetic field ($H=180$ G) and at $T_a = 573K$ without an applied field. To perform the measurement, the samples were removed from the furnace and left to cool in air to room temperature.

All the ribbons had a width of $\simeq 1.2$ mm. The quenching rate was verified by measurement of the initial permeability aftereffect $(\Delta\mu/\mu)He$ in the as-quenched state at room temperature⁴ :

Set	ribbon thickness(μ)	$(\Delta\mu/\mu)He$ (arb.units)
A	22	4.3 ± 0.9
B	20	10 ± 2
C	19	16 ± 3

The same annealing procedures were followed for various new as-quenched samples and the average values of several measurements are reported.

3. Results

The relative initial permeability aftereffect $((\Delta\mu/\mu)He)_t / ((\Delta\mu/\mu)He)_{t_0}$ in the sets of as-cast ribbons A, B and C submitted to isothermal annealing treatments at 473 K is shown in fig. 1. The reference value $((\Delta\mu/\mu)He)_{t_0}$ is taken in each

Study of kinetics of magnetic permeability...

case at $t = t_0 = 0$. Two competing $(\Delta\mu/\mu)He$ trends can be observed. At the beginning of the isothermal annealing, values for $(\Delta\mu/\mu)He$ of these samples are found to increase with t , whereas at $t > 1000s$, a different behavior is observed for each sample. For the set of ribbons A, $(\Delta\mu/\mu)He$ continues to increase, for the set B it remains almost constant and, for C, the aftereffect rapidly decreases with t . The present measurements indicate that different processes (TSRO and CSRO), producing competing effects on $(\Delta\mu/\mu)He$, occur simultaneously in low temperature aging treatments and also show that the behavior depends on the QR.

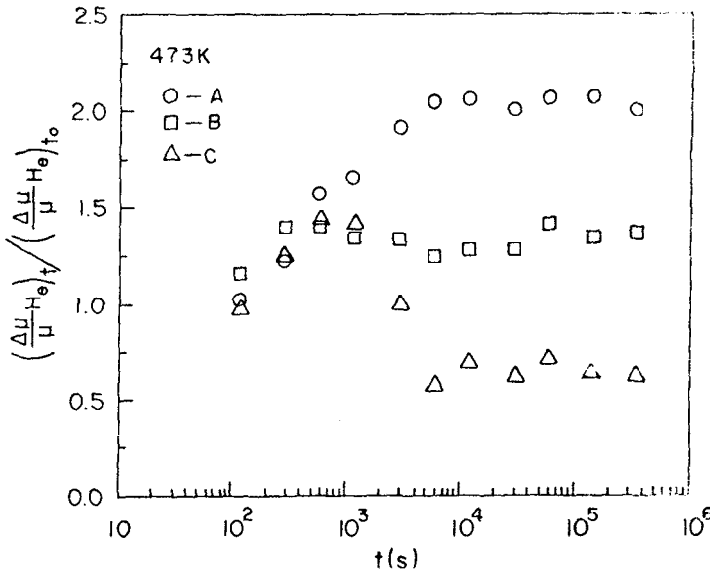


Fig.1 - Relative aftereffect of the initial magnetic permeability $((\Delta\mu/\mu)He)_t / ((\Delta\mu/\mu)He)_{t_0}$ as a function of aging time at $T_g=473K$, for the sets of ribbons A, B and C prepared at different quenching rates; $QR_A < QR_B < QR_C$.

By annealing with a magnetic field applied along the sample axis, behaviors of the $((\Delta\mu/\mu)He)_t / ((\Delta\mu/\mu)He)_{t_0}$ for as-cast ribbons are shown in fig. 2. Again, different competing effects can be observed. In this case, the annealing behaviors of the relative aftereffect of the three samples are similar, although their intensities

S. P. Cruz *f.*, M. Knobel, J. P. Sinnecker and R. Sato *Turtelli*

are much different. It is interesting to notice that the aftereffect values here obtained are much bigger than those found in fig. 1.

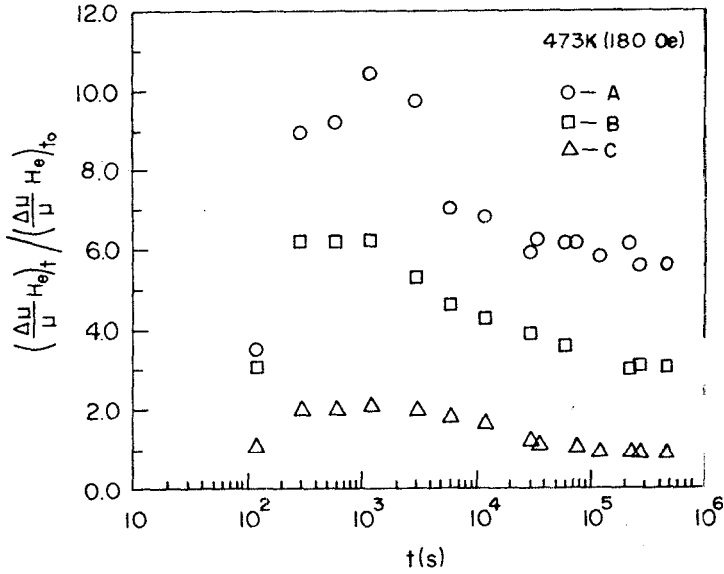


Fig.2 - Relative aftereffect of the initial magnetic permeability $((\Delta\mu/\mu)He)_t/((\Delta\mu/\mu)He)_{t_0}$ as a function of aging time at $T_a=473K$ with a longitudinal D.C.magnetic field $H=180 G$, for the sets of ribbons A, B and C.

When the samples are treated at high annealing temperature ($T_a=573K$), only a slightly decreasing branch is detected for the two slowly quenched sets (A and B) while for the fast-quenched set (C), the $(\Delta\mu/\mu)He$ practically remains unchanged in the annealing time range studied. These results show again that the behaviors of fast and slowly quenched ribbons are different. It can be observed that the aftereffect data obtained at 573K are somewhat scattered when compared to those obtained at 473K, due to fluctuations in the number of domain walls.

In particular, the development of CSRO can induce significant variations of the anisotropic distribution of different atomic species within the shell of nearest neighbors of a given atom. The presence of an induced anisotropy, ascribed

Study of kinetics of magnetic permeability...

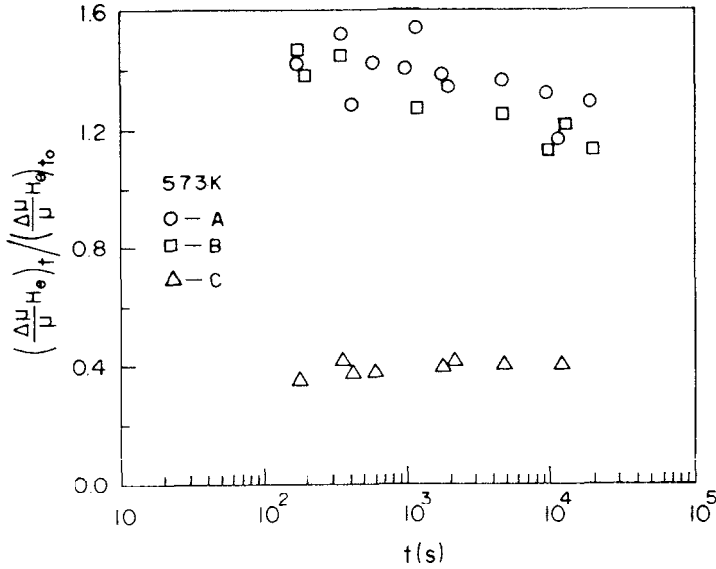


Fig.3 - Relative aftereffect of the initial magnetic permeability $((\Delta\mu/\mu)He)_t/((\Delta\mu/\mu)He)_{t_0}$ as a function of aging time at $T_a=573K$, for the sets of ribbons A, B and C.

to directional ordering of magnetic pairs, was observed in $Co_{70.4}Fe_{4.6}Si_{15}B_{10}$ alloys submitted to isothermal treatments¹². There is a direct connection between the permeability and the inverse of the induced anisotropy. Therefore, initial permeability measurements were performed simultaneously with aftereffect measurements in order to get a general view of the induction of anisotropies during different annealings.

Figures 4, 5 and 6 show the relative initial permeability $(\mu_t/\mu_{t_0}) \equiv (\mu/\mu_0)$ as a function of annealing time t , at the same conditions previously described for the figures 1, 2 and 3 respectively. These results confirm the development of an anisotropy due to annealing at a temperature and for times where the enhancements of $(\Delta\mu/\mu)He$ were observed. The values of μ were observed to steadily decrease with aging time, due to the development of directional order within the Bloch walls. More abrupt changes of μ were observed with the application of H parallel to the ribbon axis during the annealing treatments than without field, at

S. P. Cruz f., M. Knobel, J. P. Sinnecker and R. Sato Turtelli

473K. The reduction of 70-80% of μ is already observed for $t < 1000s$, as shown in fig.5. When the samples are annealed at higher T_a , 573K, the ordering processes occur more rapidly and, in the first minute of annealing, the permeability practically reaches an equilibrium value (see fig.6). The changes measured in the ribbons with slower QR are much smaller than those found with faster QR.

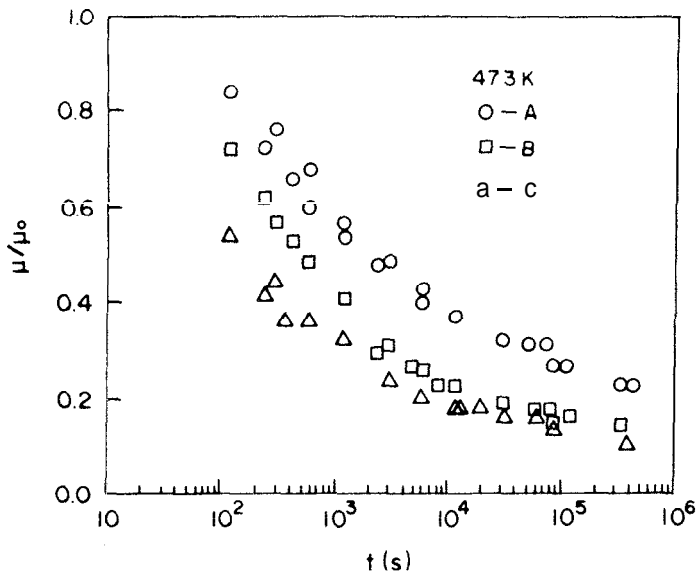


Fig.4 - Relative initial permeability μ/μ_0 as a function of aging time at $T_a=473K$, for the sets of ribbons A, B and C.

4. Discussion

Since there exists a good correlation between $(\Delta\mu/\mu)He$ and ρ (electrical resistivity)⁵, it is suggested that the same explanation given for ρ can be used to understand the $(\Delta\mu/\mu)He$ behavior. A typical increase of electrical resistivity with time is generally found in isothermal measurements performed in amorphous alloys, when some type of clustering or compositional ordering of solute atoms is present⁷. This compositional ordering occurring at rather low temperatures is

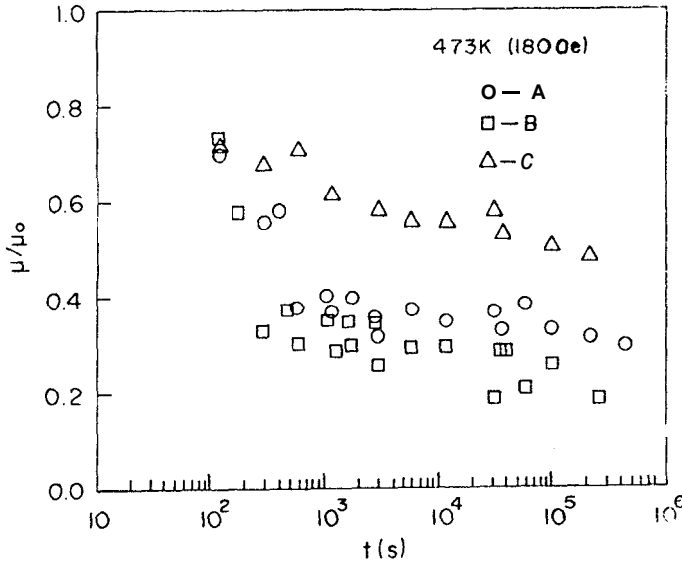


Fig.5 - Relative initial permeability μ/μ_0 as a function of aging time at $T_a=473\text{K}$, $H=180\text{ G}$, for the sets of ribbons A, B and C.

believed to take place through short range atomic diffusion, not significantly affecting the topology of amorphous bulk. At higher temperatures, more collective processes are activated, involving irreversible changes TSRO, decreasing the ρ , associated with a reduction of free volume⁷. Both ordering processes occur more rapidly in those ribbons of faster QR.⁷

Our results of isothermal annealing aftereffect measurements reported in figures 1 to 3, can be separated in two time regions. Below 1000s the aftereffect is an increasing function of t and for $t > 1000\text{s}$, $(\Delta\mu/\mu)He$ decreases with increasing t , except in the case of the ribbon prepared at lower QR (set A), when it is submitted to annealing at $T_a=473\text{ K}$. In this case, a slowly enhancement is always observed.

On the contrary, no increase of $\Delta\mu/\mu$ was observed in the $\text{Fe}_{67}\text{Ni}_{19}\text{B}_{14}$ and $\text{Fe}_{85}\text{B}_{15}$ ribbons even at low annealing temperatures¹³. These facts suggest that, in the $\text{Co}_{70.4}\text{Fe}_{4.6}\text{Si}_{15}\text{B}_{10}$ alloys, Co is the major responsible for the clustering processes, since in FeNiB and FeB alloys with no Co, only a reduction of $\Delta\mu/\mu$

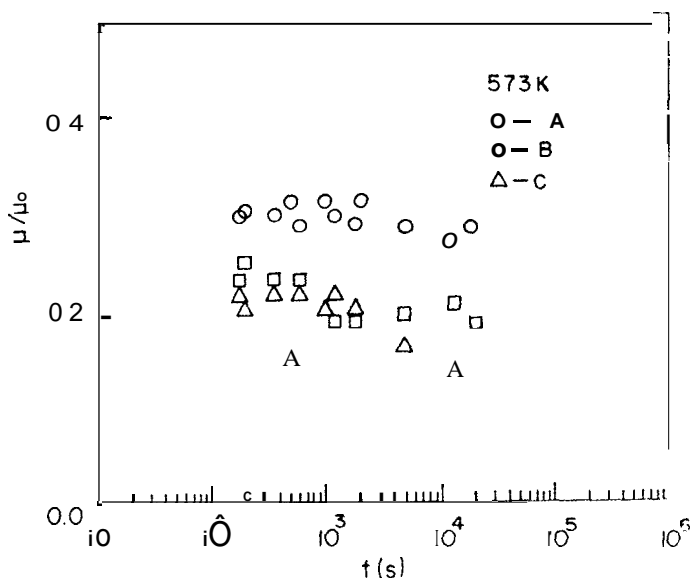


Fig.6 - Relative initial permeability μ/μ_0 as a function of aging time at $T_a=573K$, for the sets of ribbons A, B and C.

with annealing time was observed.”

The $(\Delta\mu/\mu)He$ behaviors can, therefore, be explained by assuming, in fact, the simultaneous presence of different processes responsible for structural relaxation in as-cast amorphous alloys submitted to a suitable annealing procedure.

The decrease with annealing time of the aftereffect intensity observed in the set of thermal treatments, above 10^3s , can be ascribed to a TSRO of the structure. The great difference between $(\Delta\mu/\mu)He$ vs. t curves in A, B and C sets is clearly related to different free volume contents initially present in these samples⁷.

The strong $(\Delta\mu/\mu)He$ increase observed at $t < 10^3s$ is mainly due to CSRO. The CSRO development can be seen in figs. 4 to 6. It is interesting to see the great effect that a DC magnetic field H applied during annealing has on the CSRO. As was shown in fig 5, the field H induces anisotropy more quickly, i.e., at the very beginning of annealing. For all the samples studied, the quasi equilibrium value was attained before the onset of the TSRO process. It is important to observe

Study of kinetics of magnetic permeability...

that in the fast quenched ribbons the relative aftereffect behavior obtained at $T_a=473K$, with and without an applied field during annealing are similar. On the other hand, in the behavior obtained for slowly quenched samples, the maximum relative aftereffect observed with H is in fact larger by a factor 5 than those obtained without H. A coherent shift of the relative aftereffect intensities towards higher values is observed in alloys prepared with a lower QR. This suggests that the processes of CSRO and TSRO are governed by the local concentration of the excess free volume. These results are in full agreement with the concept that the free volume existence in the amorphous alloy is effective in favoring the diffusive processes involved in short-range ordering. TSRO and CSRO. These processes are affected in the same way by the amount of free volume frozen in the alloy. These facts can be shown in fig. 7, where the proportionality between aftereffect intensities at different annealing times and QR is observed.

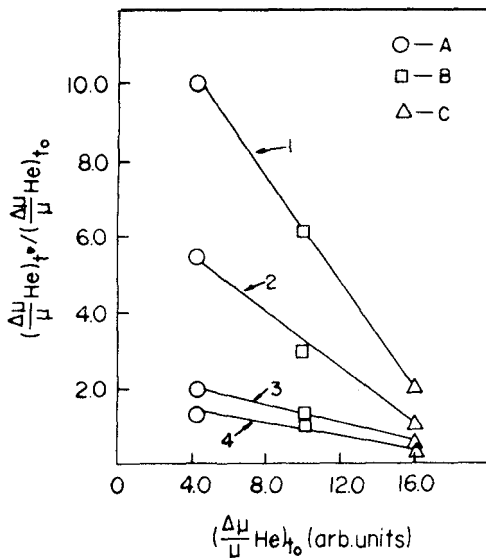


Fig.7 - The behavior of $((\Delta\mu/\mu)He)_t/((\Delta\mu/\mu)He)_{t_0}$ as a function of $((\Delta\mu/\mu)He)_{t_0}$. The values of t^+ are taken at: $t_1^+ = 10^3$ s; $t_{2,3}^+ = 4 \cdot 10^5$ s and $t_4^+ = 1.2 \cdot 10^4$ s. (1,2: $T_a=473K$, $H = 180G$; 3: $T_a=473K$; 4: $T_a=573K$).

S. P. Cruz *f.*, M. Knobel, J. P. Sinnecker and R. Sato Turtelli

In conclusion, the present work has allowed us to show that in $\text{Co}_{70.4}\text{Fe}_{4.6}\text{Si}_{15}\text{B}_{10}$ amorphous alloys the kinetics of relaxation of $(\Delta\mu/\mu)He$ is sensitive to the degree of bond-orientational disorder of the structure and to specific compositional ordering processes, such as the development of directional order for magnetic atom pairs.

Acknowledgments

The authors gratefully acknowledge Prof. Frank P. Missel and his group from Universidade de São Paulo, for the preparation of the samples.

This work was supported by FAPESP, CNPq and CAPES (Brazilian Agencies).

References

1. P. Allia and F. Vinai, *Phys. Rev. B*, 26, 6141 (1982).
2. P. Allia and F. Vinai, *Phys.Rev. B*, 33, 422 (1986).
3. H. Kronmtller, *Phil. Mag. B*, 48, 127 (1983).
4. P. Allia, F. E. Luborsky, R. Sato Turtelli and F. Vinai, *IEEE Trans. Magn.*, 17, 2615 (1981).
5. P. Allia, G. Riontino, R. Sato Turtelli and F. Vinai, *S. S. Comm.*, 43, 821 (1982).
6. M. Scott, in *Rapidly Quenched Metals III*, The Metals Society, London 1978, vol.1, pp. 198
7. G. Riontino, P. Allia and F. Vinai, *J. Non-Cryst. Sol.*, 61-62, 1365 (1984).
8. T. Egami, *J. Magn. Mag. Mat.*, 31-34, 1571 (1983).
9. P. Chieux and H. Ruppemherg, *J. Physique*, 41, C8-145 (1980).
10. T. Egami, K. Meeds, D. Srolovitz and V. Vitek, *J. Physique*, 41, C8-272 (1980).
11. R. Sato Turtelli and F. Vinai, *Rev. Bras. Fis.*, 20, 3, 219 (1990).
12. A. M. Severino, A. D. Santos and F. P. Missel, *J. Magn. Mag. Mat.*, (submitted).
13. P. Allia, R. Sato Turtelli and F. Vinai, *J. Magn. Mag. Mat.*, 39, 279 (1983).

Study of kinetics of magnetic permeability...

Resumo

Foram realizadas medidas do "aftereffect" da permeabilidade magnética inicial para três conjuntos de amostras de ligas amorfas $\text{Co}_{70.4}\text{Fe}_{4.6}\text{Si}_{15}\text{B}_{10}$ preparadas com velocidades de resfriamento diferentes. Nós efetuamos tratamentos isotérmicos para amostras "as-cast", com e sem a aplicação de campo magnético longitudinal ($H=180$ G) a **473K** e **573K**. A cinética do "aftereffect" em função do tratamento térmico pode ser entendida através de uma competição entre dois processos de relaxamento, os ordenamentos de curto alcance composicional e topológico. Ambos os processos são influenciados pela velocidade de resfriamento.